

**2RF-168 -
DERRINGER
FEDERAL RECYCLE
FACILITY ID
fVV2133637688**

Karst/Justification for use of
ERI rather than GPR in the
Burton Flats, Eddy County
New Mexico

[14744] MEWBOURNE OIL
CO

December 12, 2021

Justification for use of ERI rather than GPR in the Burton Flats, Eddy County New Mexico

The soils and alluvium of the Burton flats consist mostly of gypsum and clay minerals. While ground penetrating radar is not impossible to use in these materials, it is challenging and poses several issues. The main issue is that the clay minerals in the soil attenuate the radar signal (of a system with a center frequency high enough to resolve the typical void size in the area) to the point that the depth of investigation is generally less than 2 meters (6.6 feet). While some subsurface karst features are within that distance from the surface, the majority are between 8 and 20 meters in depth, out of range of the radar. A lower frequency radar could penetrate deeper, but not much, and the resolution wouldn't be high enough to see the smaller features. An alternative geophysical method that works quite well in these types of soils is electrical resistivity imaging (ERI). ERI at its most basic uses a set of four electrodes placed in the ground. Two electrodes are used to inject an electrical current into the ground, the other two electrodes are used to measure the voltage produced by the current. The known injected current and the measured voltage can then be used to determine the electrical resistance of the ground. Since air (as in an air-filled, subsurface void) has nearly infinite resistance, these voids show up extremely well using electrical resistivity. ERI is a complementary geophysical method to GPR and typically works very well in areas where GPR does not (as in the case of the Burton Flats). In addition to the physics involved, there are practical issues as well. The amount of time it would take to complete a comprehensive GPR survey using either a cart system, or physically moving the antennas for each measurement are prohibitive. In the former case, using a cart, the vegetation would need to be cleared prior to the survey. With the area cleared of vegetation, approximately an acre can be covered per day. In the latter case, using a unit without the cart, a measurement would have to be taken, then the antennas moved, the next measurement taken and so on. With this method, approximately a quarter of an acre per day can be covered. With ERI, no vegetation removal is required (at least in the area of the proposed infrastructure in this particular case) and between 6 and 8 acres per day can be covered. The depth to which electrical resistivity can reach is limited by the array length and the resolution of the survey is limited by the electrode spacing. Typically we use 4- to 5-meter electrode spacing which gives unambiguous results regarding subsurface voids that are between 2 to 2.5 meters in diameter or larger to a depth of 15 to 20 meters. Smaller or deeper voids still show up but can be harder to interpret. Please see the attached paper for further information.

Oklahoma Geological Survey Circular 113, 2021

Geophysical Characterization of Playa Lakes in the Gypsum Karst of Southeastern New Mexico, USA

David D. Decker

Southwest Geophysical Consulting, LLC, Albuquerque, New Mexico

Lewis Land

National Cave and Karst Research Institute, Carlsbad, New Mexico

Barbara Luke

University of Nevada, Las Vegas, Las Vegas, Nevada

ABSTRACT.—Southeastern New Mexico is host to many karst features, including caves, swallets, sinkholes, solution tubes, and springs, which are at risk of compromise by ongoing petroleum extraction. Playa lakes are shallow depressions found on gypsum bedrock in southeastern New Mexico and west Texas, and on Quaternary alluvial gravels in eastern New Mexico. These depressions are curious in that some of them are obviously linked to underground conduits via surface openings, whereas others have no such connections. These features could be cover-collapse sinkholes that have filled in with Quaternary windblown alluvium and soil, or they could be solutionally formed via pooling of rainwater, dissolution of the gypsum and re-precipitation as the water evaporates, and subsequent deflation of the unconsolidated gypsum by wind. In this study, we use field observations and three complimentary geophysical methods (ground penetrating radar, electrical resistivity imaging, and surface-wave seismic) to make inferences about the subsurface structure of these depressions and their relationship to the karst features located in and around them. The speleogenetic model that we develop from the data indicates that these playa lakes could well be karst features, as opposed to surface hydrologic features, and therefore should be treated the same way as other karst features in the region when determining the routing of linear infrastructure and the placement of resource-extraction-related pads and ponds.

INTRODUCTION

Background

Playa lakes are shallow, usually dry depressions found in soils above gypsum bedrock in the Delaware Basin in southeastern New Mexico and west Texas (Rustler and Castile Formations), the back-reef facies of the Guadalupe Reef as far north as Vaughn and Santa Rosa, New Mexico (Seven Rivers Formation), and even on Quaternary alluvial gravels in eastern New Mexico (Ogallala Formation). Many of these shallow depressions are only visible because they either host an abundance of salt-tolerant plant life or, in some cases, no plant life at all. These depressions are curious in that some of them are obviously linked to underground conduits

(caves) via surface openings (swallets), whereas others have no such features (Figure 1).

The Delaware Basin and back-reef facies of the Capitan Reef escarpment are currently undergoing rapid infrastructure build-up as petroleum exploration, discovery, and exploitation escalate. It is necessary to determine if these features provide pathways from the surface to the aquifer, and if so, to make a case for avoiding them, if possible, during pipeline and well-pad construction, road building, power-line installation, and other infrastructure development (Bureau of Land Management, 2015). Many karst features are already known in the region, including caves, swallets, cover-collapse sinkholes, caprock-collapse sinkholes, solution tubes, and springs. Currently, the recommended buffer for these

Decker, D. D.; Land, L.; and Luke, B., 2021, Geophysical Characterization of Playa Lakes in the Gypsum Karst of Southeastern New Mexico, USA, *in* Johnson, K. S.; Land, Lewis; and Decker, D. D. (eds.), *Evaporite Karst in the Greater Permian Evaporite Basin (GPEB) of Texas, New Mexico, Oklahoma, Kansas, and Colorado*: Oklahoma Geological Survey, Circular 113, p. 79-92.

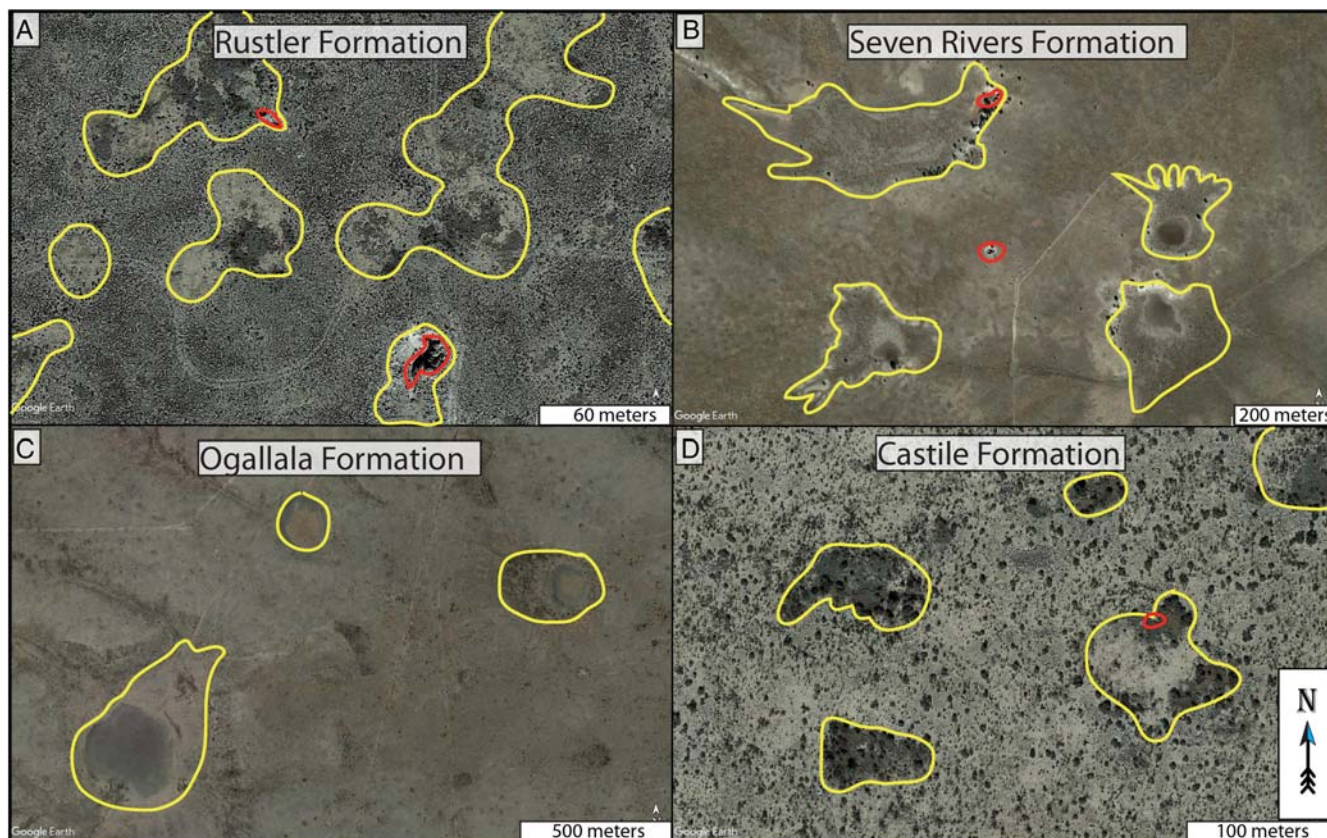


Figure 1. A. Playa lakes in the Rustler Formation (yellow outline). Several have no obvious outlet. The one on the upper left has a 2-m-diameter swallet on the eastern edge (red outline). The one in the lower right has a 4-m-diameter cave opening. B. Four playa lakes in the Seven Rivers Formation. Three of the six have no obvious outlet, whereas the fourth has a 2.5-m-diameter swallet on the eastern edge. Additionally, a 3-m-diameter sinkhole is located centrally to all four depressions. C. Three playa lakes in the Ogallala formation. None of the playa lakes in the Ogallala Formation are known to have karst features associated with them. D. Five playa lakes in the Castile Formation. Four have no karst features associated with them, the fifth has a 1-m-wide swallet in the northern edge. Notice that all of the karst features associated with a playa lake are on the perimeter.

features is determined by the likelihood of a spill or other contamination making its way to the aquifer. This buffer is currently set at 50 m for smaller karst features, or those with clogged conduit, and 200 m for larger karst features or those with open conduit (Rybacki, 2017—personal communication). What is not known is how, or even if, the playa lakes are linked to these karst features and why they are so closely associated spatially. If we find that these playa lakes should be considered karst features, rather than surface hydrologic or aeolian deflation features as some suggest, then they should be given the same buffer as other karst features in the region when determining the routing of linear infrastructure and the placement of infrastructure pads and ponds.

For this study, we chose two playa lakes with no visible outlets and a known cave that are located in the Burton Flats area (Figure 2), approximately 26 km northeast of Carlsbad, New Mexico, to conduct ground penetrating radar (GPR), electrical resistivity imaging (ERI),

and multichannel analysis of surface waves (MASW) seismic surveys. We used the known cave as a baseline (the control) for all three geophysical methods, and then we ran identical surveys over nearby playa lakes with no associated surface features to see if there was an identifiable relationship between the playa lakes and other karst features. A secondary goal, to determine the depth to which the playa lakes extend beneath the surface, was not realized but is anticipated in a future study.

Study Area

Location and Land Ownership

The study area is a 65-hectare region selected for its numerous swallets, caves, sinkholes, and playa lakes. This area is in the Burton Flats, 26 km northeast of Carlsbad, New Mexico (Figure 2), specifically in the SE SW and SW SW quarter of section 28 and the NE NW and NW NW quarter of section 33 of T19S, R29E.

Geophysical Characterization of Playa Lakes in the Gypsum Karst of Southeastern New Mexico, USA

81

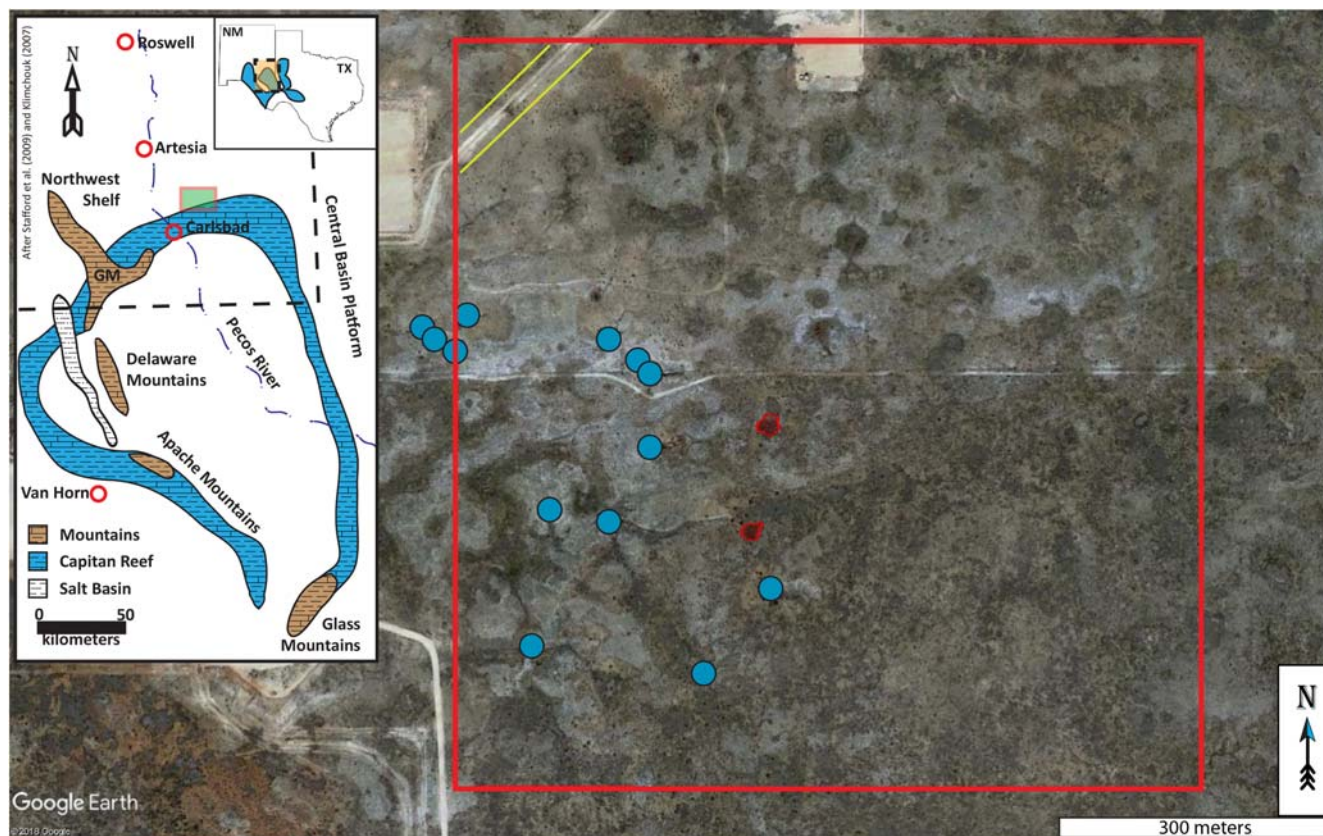


Figure 2. Study area (red square). The relationship of the study area to Carlsbad, New Mexico is shown on the regional map as a green square outlined in red. Numerous cave entrances and swallets (blue dots) and playa lakes exist in this region (playa lakes chosen for the study are highlighted in transparent red polygons). Parallel yellow lines in the northwest of the image highlight the pipeline mentioned in the text.

The land ownership of the area under study is Bureau of Land Management—Carlsbad Field Office (BLM-CFO) managed lands (36.5 hectares, southern 56%) and New Mexico State Land Office managed lands (28.5 hectares, northern 44%), with the demarcation line being the east-west two-track road near the center of Figure 2.

Land Use

The Burton Flats are presently used for cattle grazing by local ranchers, petroleum production by several large oil companies, and potash mining, predominantly by the Intrepid Potash Corporation. There are several abandoned ranch homes in the area, suggesting that historically the area was more heavily used for cattle grazing prior to the proliferation of fossil fuel extraction. There are currently only two occupied residences in the Burton Flats, neither of which are within the study area. There are numerous active well pads nearby, as well as buried pipelines that traverse the area in the far northwest corner (Figure 2). This specific area was selected for the study to minimize interference and the introduction of artifacts from radio frequency noise, pipelines, and previously disturbed soils. In the 1940s and 1950s, Burton Flats

were used by the Army Airforce as a bombing range. There are two documented sites within the Burton Flats that contain practice target ranges and a third, undocumented site (Decker, 2019) that appears to have been a live-ammunition dump. Prehistoric artifacts have been found within the Burton Flats and there are several archaeological sites within the region suggesting use by Native Americans for hunting and gathering.

Terrain and Geology

The terrain of the Burton Flats area consists of gently rolling hills, flatlands, and occasional cliffs. The area has numerous caves, sinkholes, swallets, and other minor karst features (currently over 1000 documented features [Decker, 2019; Atkinson, 2018; Belski, 2018 (personal communication)]), all aligned from southwest to northeast along the dominant lineament trend in the region; this includes the playa lakes (Figure 3). The major rock types in the area are the gypsum, dolomite, and minor sandstones of the upper Permian Rustler Formation, an evaporite facies that was deposited during the Lopingian Epoch (Ochoan Series, 259–251 Ma) (Powers and others, 1999; Swards and others, 1991).

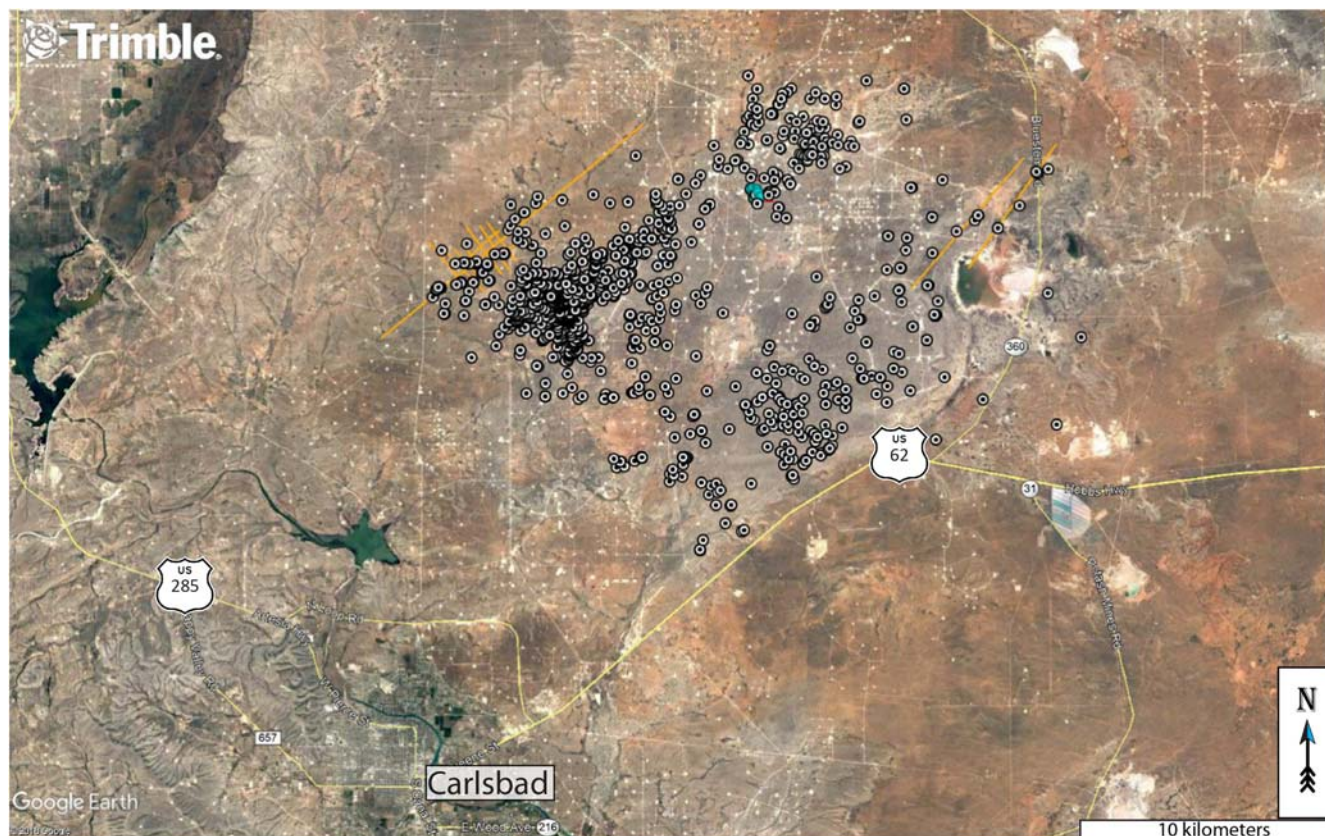


Figure 3. Karst feature distribution. Black and white dots are known or suspected karst features including caves, sinkholes, and swallets. Orange lines are tectonic lineaments. Field area is the blue triangle in the upper-central portion of the image. Note the tremendous number of white squares throughout the background image. These are all well pads, central tank batteries, or other fossil fuel extraction-related infrastructure. Background image: Google Earth. Image date: December 30, 2016. Image datum: WGS-84.

The Rustler Formation consists, in descending order, of the Forty-Niner member (gypsum), the Magenta Dolomite, the Tamarisk member (gypsum), the Culebra Dolomite, and the Los Medaños member (halitic, gypsumiferous siliciclastics) (Goodbar, 2013; Powers and others, 1999). Both the Magenta Dolomite and the Culebra Dolomite host shallow aquifers (Holt, 1997). In the study area, the local dip is to the southwest.

Caves in the Burton Flats are generally formed in the Magenta Dolomite with horizontal entrances in blind arroyos. Occasionally, a caprock-collapse sinkhole opens directly into cave passage. These sinkholes are generally not associated with the playa lakes, whereas the blind arroyos, horizontal cave entrances, and swallets are nearly always on the edges of these playa lakes (Figures 1, 4). Some playa lakes in the region also exhibit small (usually less than 1 m diameter and 50 cm deep) closed swallets at or near the center of the playa lake in soil. A nearby area that has had the surface soils removed for installation of an impoundment pond exposed solutionally enlarged fractures, small conduits, and other epikarst features (Figure 4E). The Rustler Formation is underlain by the Permian Salado Formation,

which is predominantly halite and is mined in this area by the Intrepid Potash Corporation. Numerous abandoned “wildcatter” drill holes are found throughout the Burton Flats which may intercept the Salado Formation, allowing fresh meteoric water to infiltrate and dissolve the halite.

METHODS

Ground Penetrating Radar

Ground penetrating radar reflection profiles are created by the reflection of radar energy from interfaces that are created by differences in the dielectric constant between two types of material (e.g., rock and air), or differences in water saturation levels within similar materials (Conyers, 2014). These reflection profiles are interpreted based on knowledge of the local geology, amount of recent rainfall in the area of interest, and other factors specific to the study. Depth of investigation and resolution are determined by several factors including, but not limited to, the center frequency of the antenna, soil moisture, and rock type.



Figure 4. Karst features (Decker, 2019). A and B—Caprock-collapse sinkholes. C and D—Horizontal cave entrances on the edges of playa lakes. E—Solution tube exposed by bulldozer (pole is 1.3 m in length for scale).

A Geological Survey Systems Incorporated, D400HS 350 MHz, hyperstacking antenna, and SIR-4000 control unit were used to image the top 2 m of the subsurface. A Juniper Systems Geode submeter global positioning system was used to georeference the radar profiles collected. Radar controller settings for the GPR were: 95 scans per second, 512 samples per scan, and 32 bits per sample. A dielectric constant (ϵ) of 14 was chosen based on the soil type (moist gypsite) at the survey location, and a scan window of 55.4 nanoseconds was used, giving a survey depth of 2.2 m. A 10-m-long odometer calibration and a site-specific initialization were performed prior to collecting the radar reflection profiles. A boxcar background removal filter set at 513 scans was used to remove horizontal radar reflections because our target was void space and irregular subsurface reflections. The software used for post data processing was RADAN-7 version 7.5.18.02270. During processing, a high-pass filter of 175 MHz and a low-pass filter of 740 MHz were used to filter out low and high frequency background noise, respectively. A logarithmic 8-point range gain was used to enhance signal strength at depth.

Electrical Resistivity Imaging

Electrical resistivity (ER) surveys are a common and effective geophysical method for detection of subsurface voids (e.g., Land and Veni, 2012; Land, 2013; Land and Asanidze, 2015; Land and others, 2018). The basic operating guideline for an ER survey involves generating a direct current between two metal electrodes implanted in the ground, while measuring the ground voltage between two other implanted electrodes. Given the current flow and voltage drop between the electrodes, differences in subsurface electrical resistivity can be determined and mapped. Modern resistivity surveys employ an array of multiple electrodes connected with electrical cable. Over the course of a survey, pairs of electrodes are activated by means of a switchbox and resistivity meter. The depth of investigation for a typical ER survey is approximately one-fifth the length of the array of electrodes.

Resistivity profiles illustrate vertical and lateral variations in subsurface resistivity. The presence of water or water-saturated ground will strongly affect the results of a resistivity survey by indicating a low resistivity zone. Air-filled caves or air-filled pore space provide a

distinctive high resistivity signature, since air has near-infinite resistivity, in contrast with the 10–15 orders of magnitude more conductive surrounding bedrock.

An Advanced Geosciences, Inc. SuperSting R8/IP electrical resistivity system provided by the National Cave and Karst Research Institute was used to collect resistivity data, employing a dipole–dipole array configuration. All of the ER surveys conducted at Burton Flats for this project used a 56-electrode array at 2-m electrode spacing, for a target depth of investigation of approximately 23 m.

A Topcon GR3 GPS instrument package was used to collect survey-grade GPS coordinates for each electrode. Elevation data collected during these surveys were used to correct the resistivity data for variations in topography. Electrical resistivity data were processed and inverted using EarthImager2D™ software. The EarthImager software chooses a resistivity scale unique to each inversion, designed to highlight natural conditions in the subsurface; thus, resistivity profiles from a given survey area may not have the same resistivity scale.

Multichannel Analysis of Surface Waves

The seismic testing followed the MASW method (Miller and others 1999; Park and others 1999; Xia and others 1999). A surface-coupled linear array of geophones recorded ground vibrations generated in line with the sensors by a vertical impact source. The response is dominated by Rayleigh-type surface waves, whose amplitudes are greatest at the ground surface near the source and decay with depth and with distance from the source. The wave transmission and decay pattern from each source impact are analyzed in the frequency domain using processes of forward modeling and inversion to infer a vertical layered profile of shear-wave velocity in the subsurface. This one-dimensional profile is assigned spatially to the center point of the geophone group analyzed. The measurement is duplicated, shifting source and sensor sets incrementally along the array so that the individual layered velocity profiles can be merged to create a two-dimensional vertical slice depicting shear-wave velocity beneath the array. Time-history data were collected using a system provided by the University of Nevada, Las Vegas that included a Geometrics Geode-based seismograph with 72 4.5-Hz vertical geophones coupled to the ground with spikes. The geophones were spaced 1.5 m apart to create a 106.5-m-long array. A source consisting of a rubber-band assisted weight-drop type, trailer-mounted piston. Analysis was in roll-along mode, using 24-trace gathers and 6-m offset of source to nearest sensor. The source was advanced in 3-m increments. All processing of the time histories, to include frequency-domain conversion, dispersion curve selection, inversion, and interpolation to develop the final shear-wave velocity image,

was completed using commercial software SurfSeis v.6 (Kansas Geological Survey).

Only one seismic array could be completed in the time available because of the time- and labor-intensive nature of the data gathering, inclement weather (high winds and heavy rain), and equipment issues both related and unrelated to the weather.

RESULTS

The control for this study was Owl Cave, which is located on the west side of a small playa lake at the end of a 36-m-long blind arroyo. The entrance room of the cave is 5 m wide, 12 m deep, and 6 m tall (Figure 5). A 0.5-m-diameter hole in the floor drops into a lower level which, according to the map (Figure 6), corkscrews down to a mud-floored room before pinching out. The roof of the entrance room is only 1.5–2 m beneath the surface at a point 1 m from the dripline. This location was chosen to maximize the returns from the GPR since it was not expected to see more than 2–2.5 m deep. At this location, the soil was less than 5 cm in depth; gypsum bedrock composed the remainder.

Two playa lakes were chosen for the study, both in close proximity to Owl Cave. The first (PL-01) was located 130 m east-northeast of Owl Cave. PL-01 is 1 m deep and 23 m across at the location of the survey. The second (PL-02) was located 140 m southeast of Owl Cave. Topographically, this playa lake was barely visible at approximately 5–10 cm deep and was discernable more by change in vegetation than its depth. PL-02 was 25 m across at the location of the measurements.

Ground Penetrating Radar

This study was conducted at the beginning of the local monsoon season; therefore, the ground was wet but not saturated. This condition provided the opportunity for a larger than normal difference in dielectric constant between wet soils ($14 < \epsilon < 30$) and cave passage ($\epsilon = 1$, that of air). The processed GPR data for Owl Cave show negative amplitude reflections directly above the cave as well as 20 m to the east, and another negative amplitude reflection 60 m to the west (Figure 7). These negative amplitude reflections indicate a change in dielectric constant from high to low, and in this case are consistent with changes in radar wave velocity from moist gypsum to air. However, since the noise floor is between 1 and 1.5 m in depth, we are likely only seeing the very top of the cave or just the air-filled fractures directly above the cave roof rather than the cave itself. Further to the east, the radar energy is highly attenuated by moist soil and clay in the bed of the small playa lake that feeds Owl Cave.

At PL-02, there were high amplitude, negative radar reflections just outside of and along the edges of the



Figure 5. Owl Cave entrance room. Dr. Lewis Land (left panel) and field assistants Michael Jones and David Brumbaugh (both panels) for scale. Left panel view is to the southwest. Right panel view is to the north.

playa lake (black and white reflections) that might indicate fractured rock. Lower amplitude returns (yellow) indicate a change in dielectric and most likely are where the moisture from the recent rains has infiltrated into the subsurface. This same moisture response is seen within the playa lake, along with minor attenuation of the signal because of clay and soil.

Ground penetrating radar survey was not conducted over PL-01 because of the amount of vegetation and the local topographic relief.

Electrical Resistivity

High resistivity anomalies may represent either air-filled void space in the subsurface (caves or potential sinkholes) or brecciated/leached zones in gypsum bedrock with air-filled pore space (Land and Asanidze, 2015). Laterally continuous layers of high or low resistivity may reflect near-surface stratigraphy, such as gypsum or dolomite beds (generally higher resistivity), or

mudstone/shale layers (lower resistivity). Very near-surface low resistivity layers may indicate water-saturated fine-grained sediment accumulated in surface depressions. In the case of Owl Cave, both of the void spaces that underlie the array show up unequivocally, along with another possible cave to the west. The low resistivity clays of the Owl Cave playa lake are visible just to the east at ground level (BF-1, Figure 8, upper panel).

PL-02 (BF-2 in Figure 8, lower panel) also shows the low resistivity clay-rich playa floor along with what we interpret as a possible fluid flow channel along the edges and fractured or brecciated rock beneath, based on resistivity values that are high (22,000 Ohm-m), but not as high as Owl Cave (100,000 Ohm-m). We see a similar pattern, less pronounced, and with lower overall resistivity contrasts at PL-01 (Figure 9, upper panel). Results show a possible fluid flow conduit along the western edge as well as the very low resistivity clays of the playa

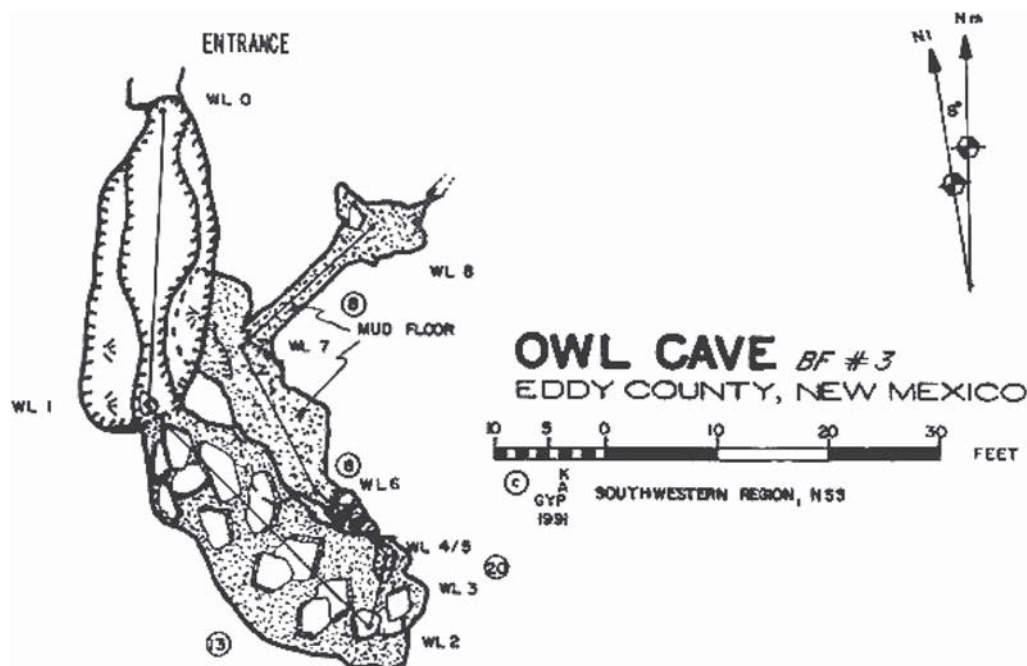


Figure 6. Owl Cave (Knapp, 1991). When overlain on the satellite imagery (see Fig. 13) the upper-level passage wraps around the outer edge of the playa lake, whereas the lower passage trends linearly along the dominant regional tectonic fractures.

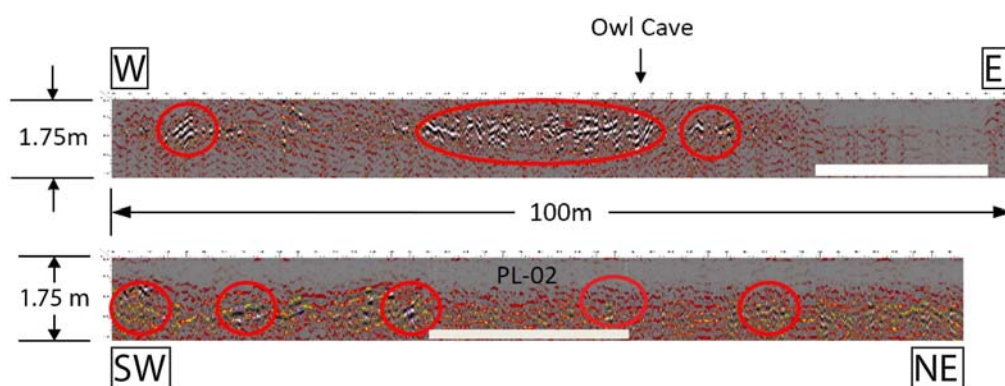


Figure 7. Radar reflection profiles. Upper panel is over Owl Cave. Lower panel is over PL-02. Red ellipses indicate high-amplitude, negative reflections. White bar on the bottom of each panel indicates the extent of the playa lake associated with that radar transect.

lake. We also ran a resistivity line along the surface in an area that had no known karst features or playa lakes (Figure 9, lower panel). Here we saw the locally southwest dipping gypsum beds and no evidence for voids or for fluid flow paths.

Multichannel Analysis of Surface Waves

Results from the seismic testing over PL-02 are shown in Figure 10. Twenty-five vertical shear-wave velocity profiles developed at 3-m spacing were interpolated to generate the single image which represents 72 m laterally and ~30 m vertically. The top surface was adjusted

before interpolation to reflect topography. Velocities range from about 200 to 800 m per second, with higher values appearing in isolated patches at depth.

Shear-wave velocities are representative of material stiffness and density. Layered soil and rock strata associated with undisturbed sedimentary deposition and subsequent weathering would present a similarly layered shear-wave velocity image, following the dip of the strata. The image beneath the playa lake does not follow this pattern. Instead, it shows distinctly lower velocity directly beneath the surface depression, extending to ~3–6 m deep. Velocities increase to about 700 m per second at about 10 m depth. Beneath that depth are seen

Geophysical Characterization of Playa Lakes in the Gypsum Karst of Southeastern New Mexico, USA

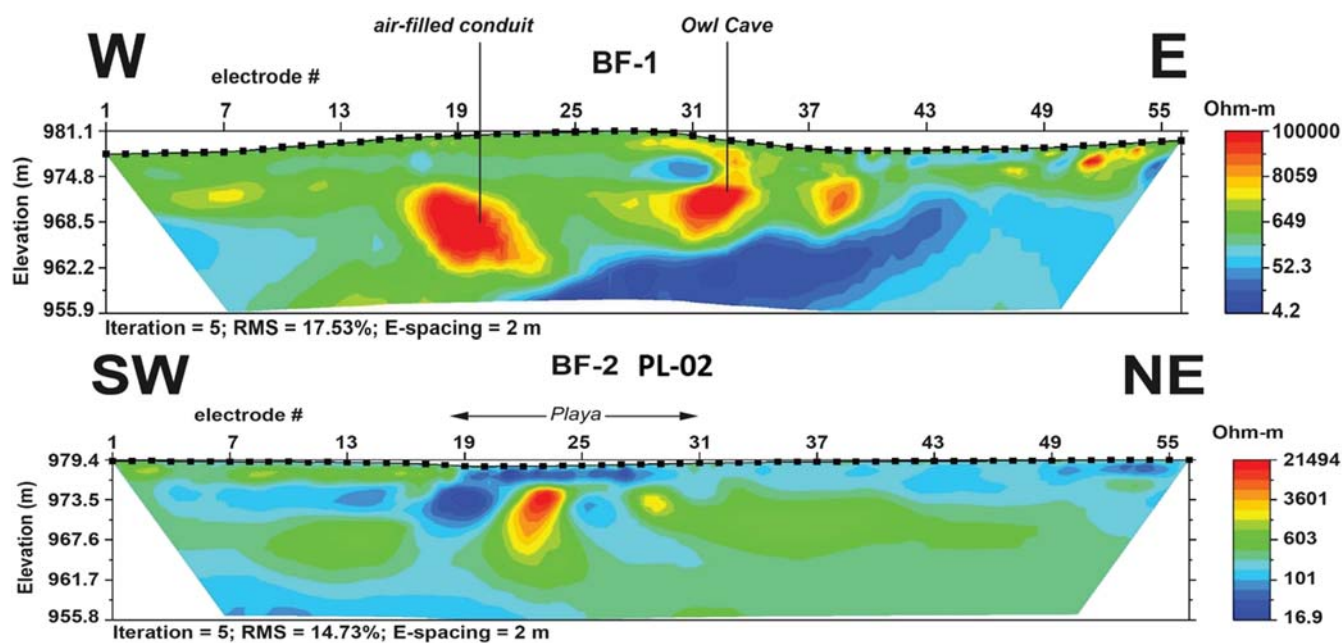


Figure 8. Upper panel: resistivity line BF-1 over Owl Cave. Lower panel: resistivity line BF-2 over PL-02. Notice that the color scales are different.

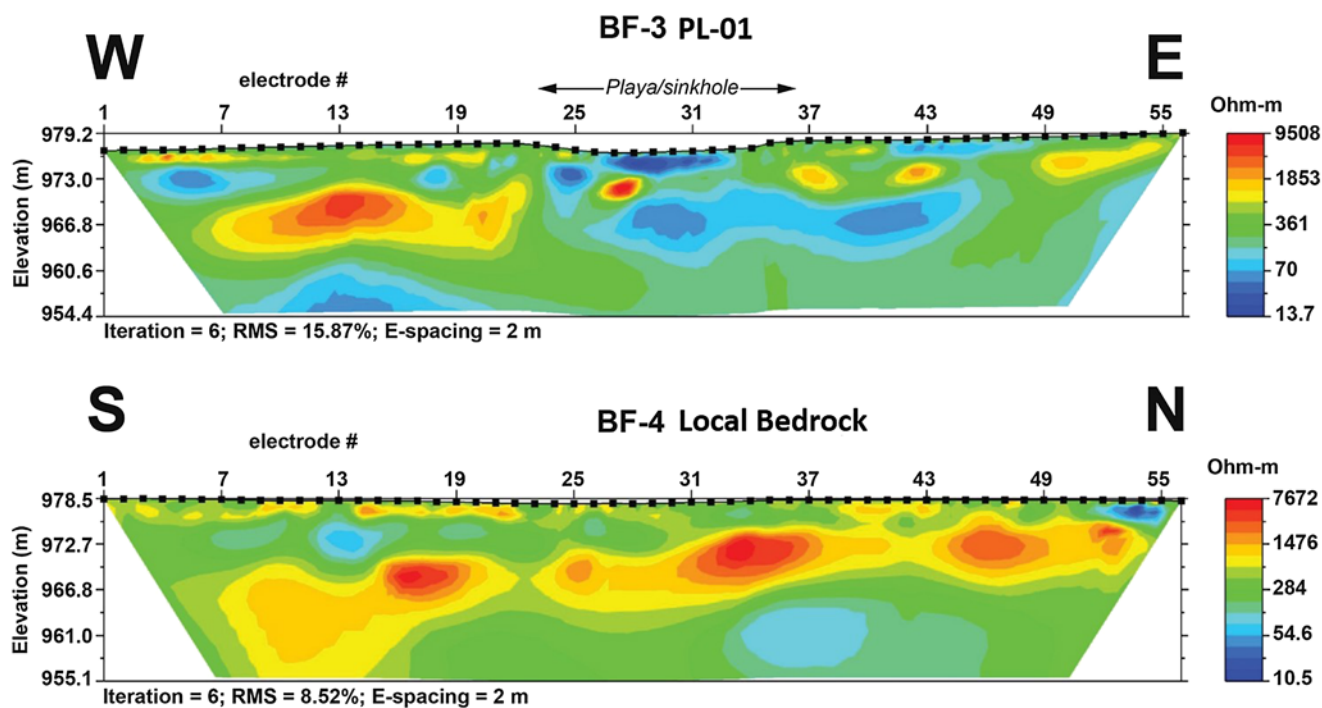


Figure 9. Upper panel: resistivity line BF-3 over PL-01. Lower panel: resistivity line BF-4 over local bedrock with no karst features. Notice that the color scales are similar, but not the same. The panels show the strata dipping gently toward the southwest.

lateral velocity fluctuations consistent with disturbed ground, possibly broken rock and uncemented matrix associated with rock stoping/brecciation. The highest velocities in the image appear beyond the edges of the playa, perhaps beyond the zone of disturbance from a

breccia pipe. However, the velocity fluctuations are not limited to the zone directly adjacent to the playa.

When interpreting the results of a surface-wave survey, one should bear in mind that confidence is highest at shallow depths, where the wave energy concentrates,

88

David D. Decker, Lewis Land, and Barbara Luke

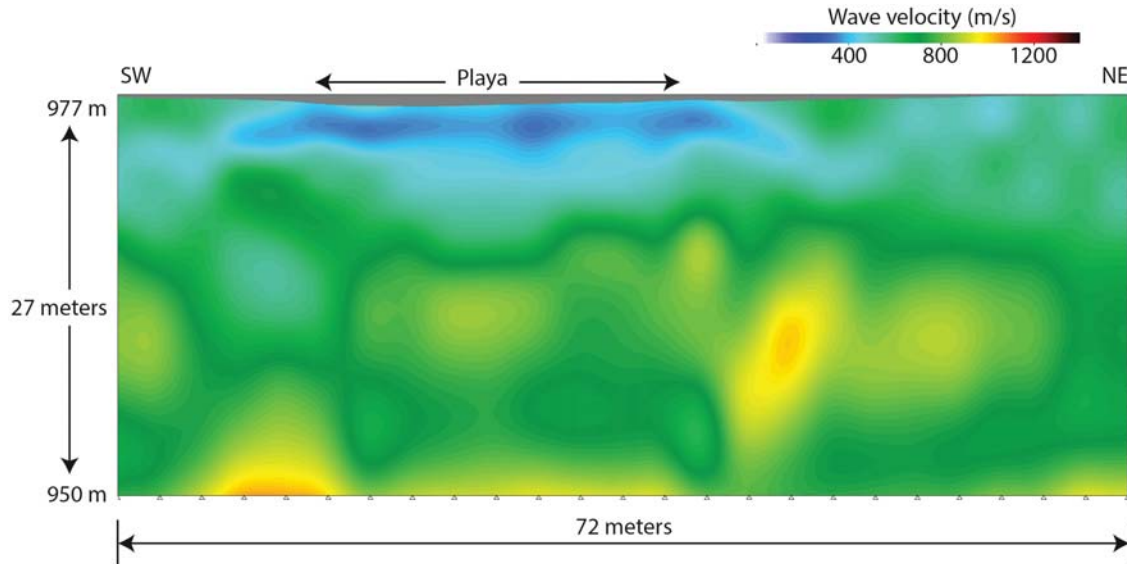


Figure 10. MASW results over PL-02.

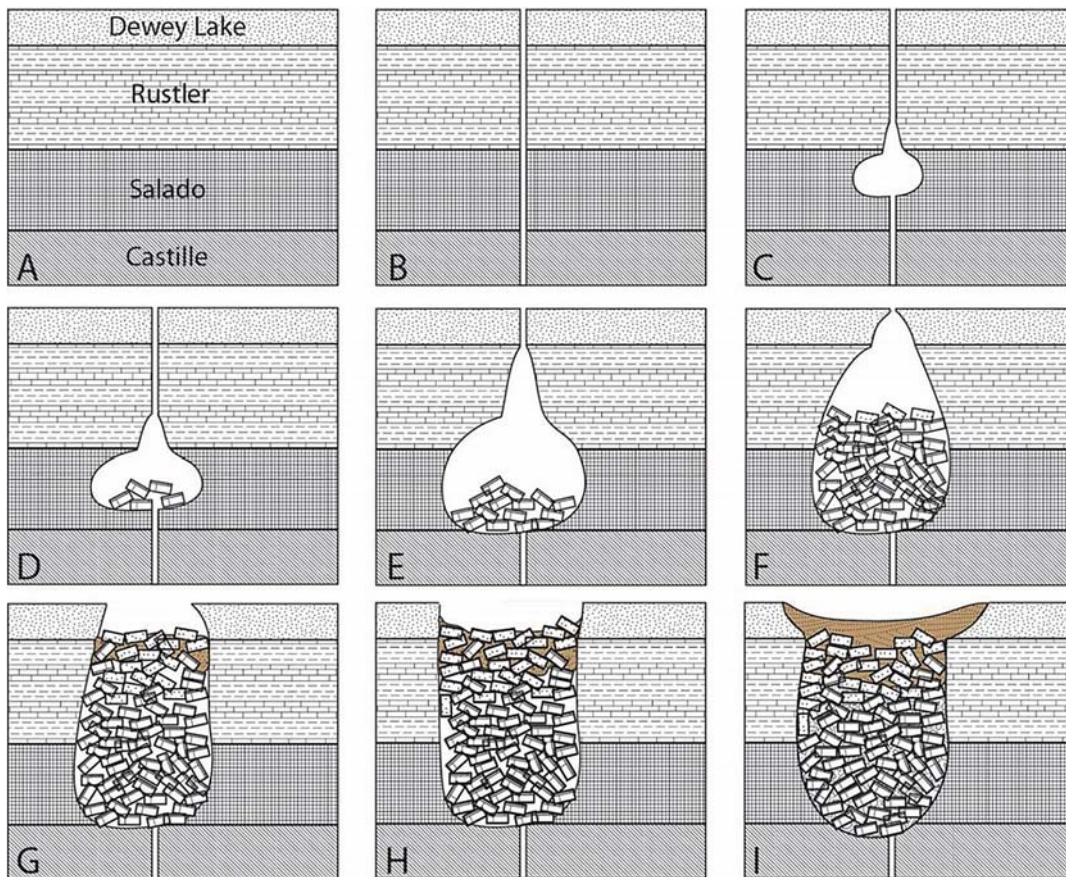


Figure 11. Hypothesis 1. Progression of sinkhole development. A: Prekarst formation. B: Fracture or drill hole allows fresh meteoric water to penetrate to the Salado Formation. C: Dissolution of halite begins. D–F: Stopping occurs. G: Void breaches surface forming sinkhole. H: Windblown deposits begin to fill brecciated sinkhole. I: Playa lake forms. Not shown: secondary voids begin to form along and within the brecciated edge of the playa lake.

Geophysical Characterization of Playa Lakes in the Gypsum Karst of Southeastern New Mexico, USA

89

and away from the ends of the array, where data density declines.

DISCUSSION

We consider two hypotheses for the formation of these playa lakes. In the first (Figure 11), playa lakes are formed by dissolution at depth, possibly as deep as the Salado Formation. Voids are formed by this dissolution and stope to the surface, where the newly created breccia pipes are slowly infilled by aeolian and biological processes. Fractures formed by the collapse of the surface allow water infiltration, which dissolves conduits and voids in the gypsum bedrock along the edges of the playa lakes forming the caves and swallets during a secondary speleogenetic episode. In this case, we would expect the geophysical data to show a demarcation between the edge of the breccia pipe and the surrounding strata.

In the second hypothesis (Figure 12), playa lakes are solutionally formed via pooling of rainwater in terrain-induced topographic low areas. Dissolution of gypsum at the surface within these areas begins when meteoric

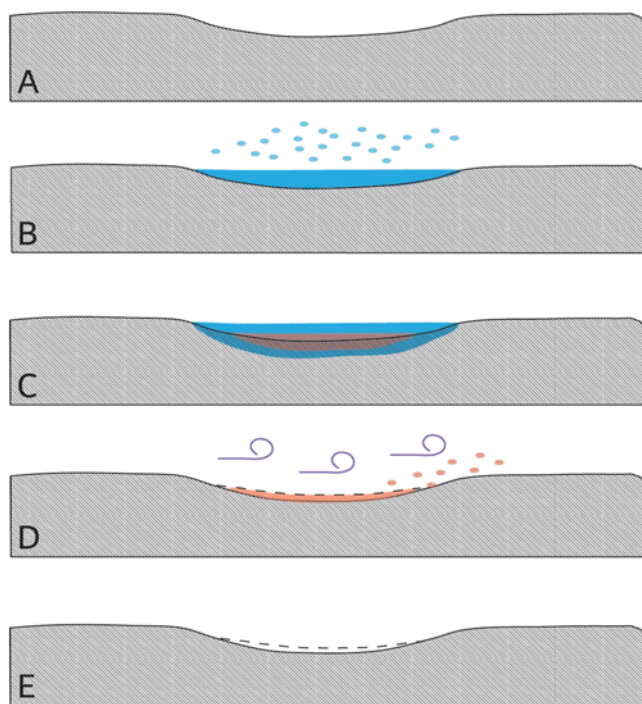


Figure 12. Hypothesis 2. A: Slight topographic depression in gypsum bedrock. B: Meteoric water fills the depression. C: Dissolution of gypsum (orange) occurs. D: As water evaporates or drains, gypsum is deposited as crust or dust and is deflated by wind. E: The depression becomes deeper (original surface denoted by dashed line). Not shown: voids already present in the subsurface are truncated by the growing depression. Note: Unlike in hypothesis 1, there is no boundary beneath the playa lake.

water undersaturated in gypsum pools in these low spots and is re-precipitated as a gypsite powder as the water evaporates. Subsequent deflation of the unconsolidated gypsum by wind occurs, thereby preferentially making the area available for more rainwater collection, enhancing the process. As dissolution at the surface progresses, voids and conduits already present in the subsurface are truncated by the edges of the playa lake as it grows deeper. In this case, we would expect to see no boundary between the playa lake proper and the surrounding strata, nor any brecciated material directly underneath.

When the results of the ERI and GPR data over Owl Cave are studied, the void spaces (and fractures above them) stand out prominently, as do the clay-filled portions of the associated playa lake. Alignment of the resistivity and radar profiles with the satellite imagery and superimposed cave map (Figure 13) clearly demonstrates that mapped voids in the subsurface coincide with resistivity and radar anomalies. The playa lake at the east end of both profiles displays as low resistivity and attenuated radar energy, as expected. We conducted postprocessing of the ERI and GPR data before the cave map became available to us; thus, the passage to the east of the main conduit was unknown when the postprocessing was done. This serendipitous sequence of events provided excellent ground truth for the study area.

When the results of all three methods are compared for PL-02 (Figure 14), consistent features are evident throughout all three profiles. In the resistivity profile, high resistivity areas that are interpreted as fractures exist near the edges of the playa lake (orange bars in Figure 14). Low resistivity areas near the surface are verified clay-rich soil, whereas those that trend downward from the surface of the playa lake are interpreted to be hydrologic conduits that funnel water into the subsurface. This same set of features can be seen in the PL-01 resistivity profile (Figure 9, upper panel). In the radar reflection profile, the tops of these same features can be seen as negative amplitude radar returns. This is most likely caused by air- or soil-filled fractures. At the surface of the playa lake, mild attenuation is occurring, consistent with the clay-rich soil. In the seismic shear-wave velocity profile, areas of low wave speed (blue) are consistent with the shallow fine-grained soils at the surface depression of the playa, and areas of high velocity (yellow) are consistent with undisturbed bedrock outside of the playa and discrete breakdown blocks beneath the playa (Figure 14).

Based on these results, we propose the following model for the formation of a playa lake: Dominant southwest to northeast tectonic trends in the region provide pathways for meteoric water to percolate through the subsurface to the Salado Formation, where it dissolves the soluble bedrock forming a void. This void then stopes upward forming a breccia pipe through the Rustler

90

David D. Decker, Lewis Land, and Barbara Luke

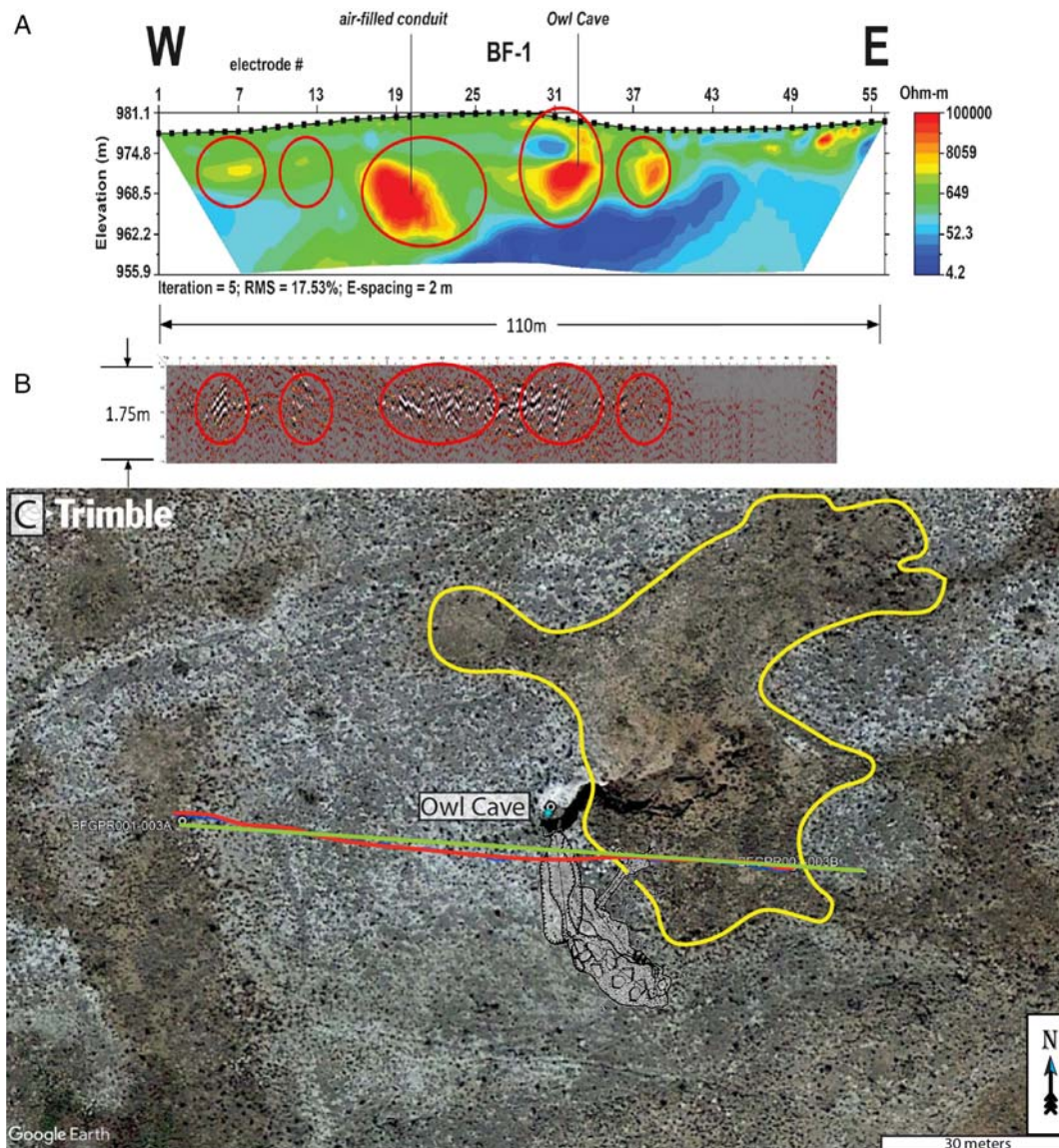


Figure 13. Resistivity versus radar versus Owl Cave map. The ERI profile (green line) is 110 m in length (vertical scale exaggerated 2.2:1) and the GPR profile (red line) is 100 m in length. The vertical scale on the GPR image is highly exaggerated (63:1). The presence of the lower passage was unknown to the authors prior to conducting the geophysical surveys. Cave map overlays from Knapp (1991).

Formation which, if it reaches the surface, creates a caprock-collapse sinkhole. This sinkhole fills in through time with aeolian sediment and locally derived soils forming the playa lake. Concurrently, the fracture rim and breccia beneath the surface of the playa lake act as highly permeable pathways, rapidly diverting water that collects in the playa lake to the subsurface along preferential flow paths, creating a secondary speleogenetic event. Since gypsum is easily dissolved in fresh water [$K_{sp} = 4.93 \times 10^{-5}$ versus limestone $K_{sp} = 3.36 \times 10^{-9}$; Lide (2000)], these preferential flow routes enlarge along the outside edges of the playa lake relatively quickly from the surface downward. Eventually the conduit breaks

through to the tectonic fractures and allows the meteoric water to begin to dissolve the gypsum along these trends. Our review of maps of nine out of ten of the known caves within the study area (Figure 2) supports this model.

Our results do not support the second hypothesis involving surface deflation, in that there are clearly subsurface structural anomalies evident in the results of all three methods. This is not consistent with a model in which there has been no disturbance of the bedrock below the playa lakes.

Our findings indicate that these playa lakes should be considered as part of the karst feature catalog and treated as such when planning for future development in the

Geophysical Characterization of Playa Lakes in the Gypsum Karst of Southeastern New Mexico, USA

91

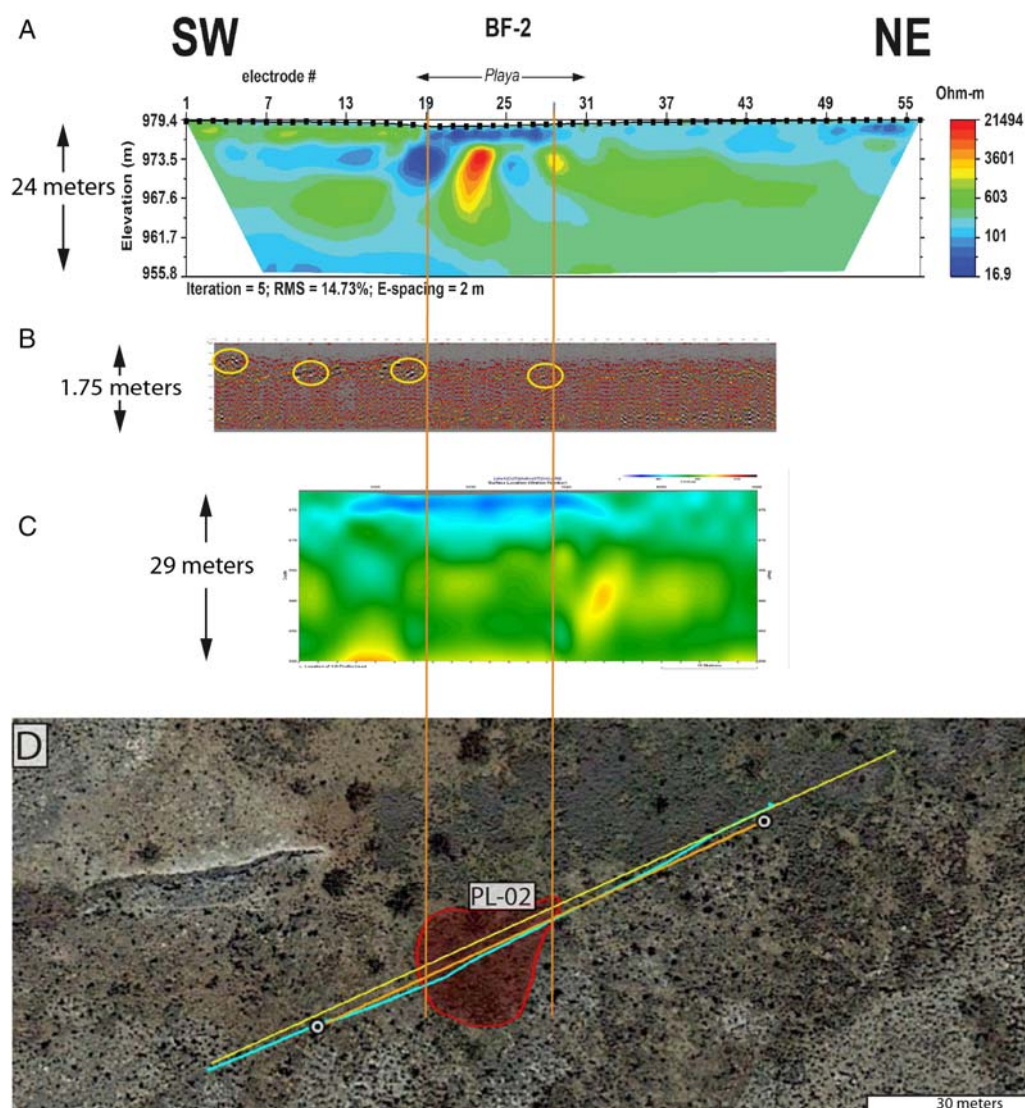


Figure 14. PL-02 resistivity, radar, and seismic comparison. The ERI profile (yellow line) is 110 m in length (no vertical exaggeration), the GPR profile (blue line) is 90 m in length (vertical scale exaggerated 63:1), and the MASW profile (orange line) is 72 m in length (no vertical exaggeration). The red transparent area on the satellite image shows the location of the playa lake.

Burton Flats and other areas of gypsum bedrock that support these features. Future planned research includes at least one of the authors visiting the interior of the caves within the study area to verify the maps and gain further insight into the formation of these karst features. Additionally, six pseudo three-dimensional resistivity surveys are planned south of the original study area where the BLM-CFO is considering implementing an Area of Critical Environmental Concern (ACEC). This ACEC contains numerous small caves, swallets, and playa lakes. Each survey area will cover approximately 3.6 hectares and extend to between 30 and 50 m in depth. Ground truth of these results will include drilling selected high resistivity areas to test for the existence of voids.

SUMMARY

Three complimentary geophysical methods were used in this study. Results indicate distinct boundaries around, and the possibility of fractured rock beneath, the two playa lakes studied.

We interpret our results to indicate the soft soils of the playa lake, disturbed bedrock, and possible minor void spaces (fractures). High resistivity areas in the ERI image for PL-02 correspond to highly reflective (negative amplitude) areas in the GPR image and low shear-wave velocity regions in the seismic image (all of which are consistent with geologic disturbance below the playa lake). Low resistivities and low velocities along the outside edge of the playa lake may indicate hydrologic

conduits. These interpretations are consistent with the fractured perimeter and collapse rubble described in the caprock-collapse sinkhole hypothesis which would indicate that the playa lakes in this study are karst related and should be protected accordingly.

ACKNOWLEDGEMENTS

We wish to thank the organizations that provided monetary support, including the Robertson Association, the National Speleological Society, and the Cave Conservancy Foundation. Additionally, we wish to thank the organizations that provided material and personnel support, including the National Cave and Karst Research Institute, the University of Nevada, Las Vegas, the Sandia Grotto of the National Speleological Society, and Southwest Geophysical Consulting, LLC.

REFERENCES CITED

- Atkinson, G., 2018, unpublished data, New Mexico Cave Survey Database.
- Bureau of Land Management, 2015, Cave and karst resources management: BLM Manual H-8380-1, Denver, CO, 59 p.
- Conyers, L.B., 2014, Interpreting ground penetrating radar for archaeology: Routledge Press, 220 pp.
- Decker, D.D., 2019, unpublished data, Southwest Geophysical Consulting, LLC, Cave and Karst Survey Database.
- Goodbar, J.R., 2013, Solution mining and the protection of karst groundwater supplies in Burton Flats, southeast New Mexico, USA, *in* Land, L., and Joop, M., eds., 20th National Cave and Karst Management Symposium: National Cave and Karst Research Institute, Carlsbad (NM), p. 13-18.
- Holt, R.M., 1997, Conceptual model for transport processes in the Culebra Dolomite Member, Rustler Formation: Sandia National Laboratories, SAND97-0194, p. 162.
- Knapp, R., 1991, Burton Flats – Area #1, *in* Belski, D., ed., Gypsum Karst Project, Vol. 2, p. 37-39.
- Land, L., 2013, Geophysical records of anthropogenic sinkhole formation in the Delaware Basin region, southeast New Mexico and west Texas, USA: Carbonates and Evaporites, Vol. 28 (1-2), p. 183-190.
- Land, L., and Asanidze, L., 2015, Roll-along resistivity surveys reveal karstic paleotopography developed on near-surface gypsum bedrock, *in* Doctor, D.H., Land, L., and Stephenson, J.B., eds., Proceedings of the Fourteenth Multidisciplinary Conference on Sinkholes and the Engineering and Environmental Impact of Karst, Rochester, Minnesota: National Cave and Karst Research Institute, Carlsbad (NM), Symposium 5, p. 365-370.
- Land, L., Cikoski, C.K., and Veni, G., 2018, Sinkholes as transportation and infrastructure geohazards in mixed evaporite-siliciclastic bedrock, southeastern New Mexico, *in* Sasowsky, I.D., Byle, M.J., and Land, L., eds., Proceedings of the Fifteenth Multidisciplinary Conference on Sinkholes and the Engineering and Environmental Impact of Karst, Shepherdstown, WV: National Cave and Karst Research Institute, Carlsbad (NM), Symposium 7, p. 367-377.
- Land, L., and Veni, G., 2012, Electrical resistivity surveys of anthropogenic karst phenomena, southeastern New Mexico: New Mexico Geology, Vol. 34 (4), p. 117-125.
- Lide, D.R., 2000, Handbook of chemistry and physics: CRC Press, Vol. 81, Ch. 8, p. 112.
- Miller, R.D., Xia, J., Park, C.B., and Ivanov, J.M., 1999, Multichannel analysis of surface waves to map bedrock: The Leading Edge, Vol. 18 (12), p. 1392-1396.
- Park, C., Miller, R.D., and Xia, J., 1999, Multi-channel analysis of surface waves: Geophysics, Vol. 64 (3), p. 800-808.
- Powers, D.W., and Holt, R.M., 1999, The Los Medaños Member of the Permian (Ochoan) Rustler Formation: New Mexico Geology, Vol. 21, No. 4, p. 97-103.
- Sewards, T., Glenn, R., and Keil, K., 1991, Mineralogy of the Rustler Formation in the WIPP-19 Core: Sandia National Laboratories, SAND87-7036, p. 98.
- Xia, J., Miller, R.D., and Park, C.B., 1999, Estimation of near-surface shear-wave velocity by inversion of Rayleigh waves: Geophysics, Vol. 64 (3), p. 691-700.



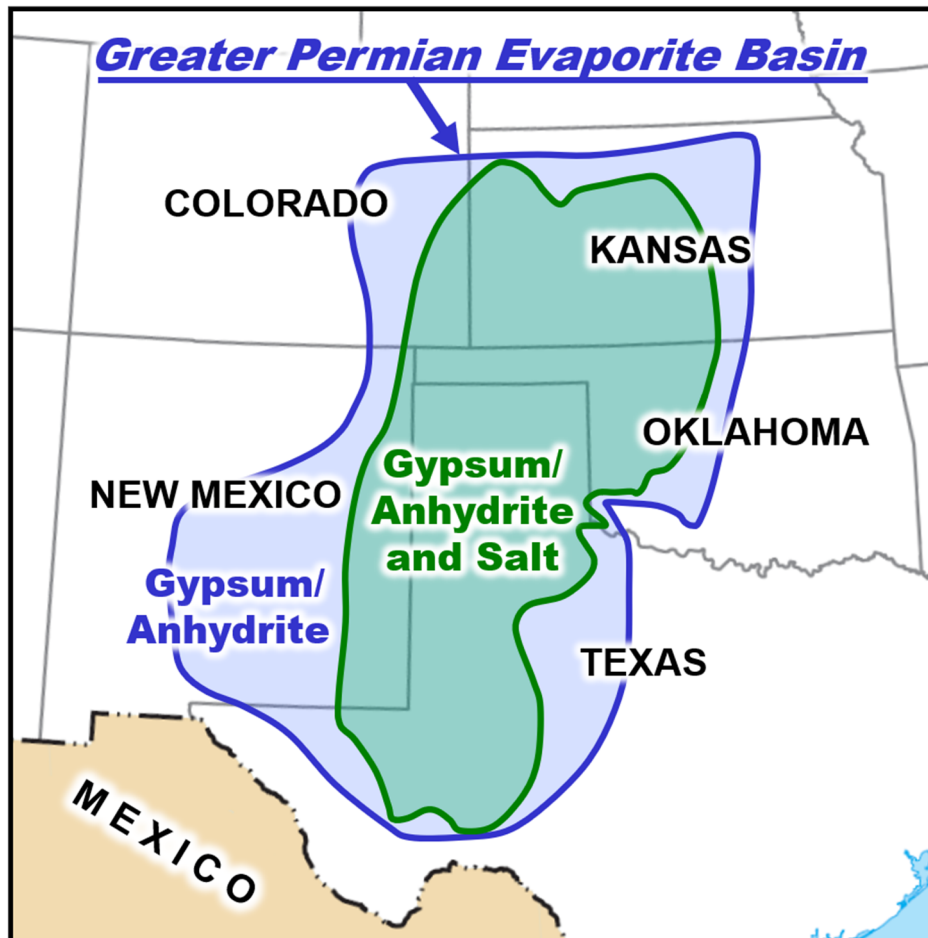
Oklahoma Geological Survey
Nicholas W. Hayman, *Director*

Circular 113
ISSN 0078-4397

Evaporite Karst in the Greater Permian Evaporite Basin (GPEB) of Texas, New Mexico, Oklahoma, Kansas, and Colorado

Kenneth S. Johnson, Lewis Land, and David D. Decker; *Editors*

2021



The University of Oklahoma
Norman, Oklahoma

District I
 1625 N. French Dr., Hobbs, NM 88240
 Phone:(575) 393-6161 Fax:(575) 393-0720
District II
 811 S. First St., Artesia, NM 88210
 Phone:(575) 748-1283 Fax:(575) 748-9720
District III
 1000 Rio Brazos Rd., Aztec, NM 87410
 Phone:(505) 334-6178 Fax:(505) 334-6170
District IV
 1220 S. St Francis Dr., Santa Fe, NM 87505
 Phone:(505) 476-3470 Fax:(505) 476-3462

State of New Mexico
Energy, Minerals and Natural Resources
Oil Conservation Division
1220 S. St Francis Dr.
Santa Fe, NM 87505

CONDITIONS
 Action 65219

CONDITIONS

Operator: MEWBOURNE OIL CO P.O. Box 5270 Hobbs, NM 88241	OGRID: 14744
	Action Number: 65219
	Action Type: [C-147] Water Recycle Long (C-147L)

CONDITIONS

Created By	Condition	Condition Date
vvenegas	None	12/6/2021